

Phenomenology of the minimal $B - L$ extension of the Standard Model: the Higgs sector

Lorenzo Basso,^{1,2} Stefano Moretti,^{1,2} and Giovanni Marco Pruna^{1,2}

¹*School of Physics & Astronomy, University of Southampton,
Highfield, Southampton SO17 1BJ, UK*

²*Particle Physics Department, Rutherford Appleton Laboratory,
Chilton, Didcot, Oxon OX11 0QX, UK*

Abstract

We investigate the phenomenology of the Higgs sector of the minimal $B - L$ extension of the Standard Model. We present results for both the foreseen energy stages of the Large Hadron Collider ($\sqrt{s} = 7$ and 14 TeV). We show that in such a scenario several novel production and decay channels involving the two physical Higgs states could be accessed at such a machine. Amongst these, several Higgs signatures have very distinctive features with respect to those of other models with enlarged Higgs sector, as they involve interactions of Higgs bosons between themselves, with Z' bosons as well as with heavy neutrinos.

I. INTRODUCTION

In the past years, major efforts have been devoted to the realisation of the Large Hadron Collider (LHC), the largest and most powerful running collider in the world. One of its scopes is discovering the means of generating masses for all known (and possibly new) particles.

As a matter of fact, while it is widely accepted that the way of realising the aforementioned mass generation is represented by the Higgs Mechanism, there is still no experimental evidence of any Higgs boson.

As for the models implementing the Higgs mechanism, the Standard Model (SM) is based on just one complex Higgs doublet consisting of four degrees of freedom, three of which, after spontaneous Electro-Weak Symmetry Breaking ($EW\!SB$), turn out to be absorbed in the longitudinal polarisation component of each of the three weak gauge bosons, W^\pm and Z , whilst the fourth one gives the physical Higgs state h (for a detailed “anatomy” of the Higgs mechanism in the SM see [1]).

Despite the SM provides a beautiful explanation for most known particle phenomena, it turns out to be unsatisfactory from several points of view. Apart from some feeble hints of the SM inadequacy coming from precision tests, it does not produce a viable dark matter candidate, it does not incorporate dark energy, it does not provide enough CP violation to explain the baryonic matter-antimatter asymmetry of the universe and, finally, it cannot describe the experimentally observed evidence of neutrino oscillations.

To stay with the latter aspect, and following a bottom-up approach, one can attempt to remedy this issue through a minimal extension of the SM : the so-called minimal $B-L$ model (see [2, 3] and [4]). Such a scenario consists of a further $U(1)_{B-L}$ gauge group in addition to the SM gauge structure, three right-handed neutrinos (designed to cancel anomalies) and an additional complex Higgs singlet responsible for giving mass to an additional Z' gauge boson. Therefore, the scalar sector is made of two real CP-even scalars, that will mix together.

In this theoretical framework, following the $B-L$ symmetry breaking, the right-handed neutrinos can acquire a Majorana mass of the order of the TeV scale ($\sim B-L$ symmetry breaking Vacuum Expectation Value (VEV)), and this can in turn explain the smallness of the light-neutrinos masses via the Type I see-saw mechanism (see [5–10]).

Finally, it is important to note that in this model the $B-L$ breaking can take place at the TeV scale, i.e., far below that of any Grand Unified Theory (GUT), thereby giving rise

to new and interesting phenomenology at present and future particle accelerators [11–16].

In the present work we study the phenomenology at the Large Hadron Collider (LHC) of the scalar sector of the minimal $B - L$ model. We will present production cross sections, Branching Ratios (BRs) and event rates for the $B - L$ Higgs bosons, highlighting the analogies and differences with respect to the SM case and other models that show a similar phenomenology in the Higgs sector (as the scalar singlet extension of the SM , see [17–22]), and we will use these results to introduce new Higgs boson signatures at the LHC, that could be the hallmark of the model considered here: e.g., four lepton decays of a heavy Higgs boson via pairs of Z' gauge bosons (which, e.g., in the SM also occurs via W^+W^- and ZZ but in very different kinematic regions), light Higgs boson pair production via the heavy Higgs boson (forbidden, e.g., over the currently allowed parameter space of the Minimal Supersymmetric Standard Model ($MSSM$)) and heavy neutrino pair production via a light Higgs boson (yielding, e.g., very exotic and clean like-sign dilepton signatures, with or without jets).

This work can be seen as the continuation of the studies started in Refs. [12, 15, 16], where we dealt with the other new sectors of the model (i.e., the Z' gauge boson and the heavy neutrino ones), and relies on the results of Refs. [23–25] where the Higgs parameter space of the minimal $B - L$ model was studied in detail by accounting for all experimental and theoretical constraints.

This paper is organised as follows: in the next section we describe the model in its relevant (to this study) parts, in the following one we describe the details of the analysis carried out, in section IV we present our numerical results, then we conclude in section V.

II. THE MODEL

The model under study is the minimal $U(1)_{B-L}$ extension of the SM (see Refs. [12, 23, 24] for conventions and references), in which the SM gauge group is augmented by a $U(1)_{B-L}$ factor, related to the Baryon minus Lepton ($B - L$) gauged number. In the complete model, the classical gauge invariant Lagrangian, obeying the $SU(3)_C \times SU(2)_L \times U(1)_Y \times U(1)_{B-L}$ gauge symmetry, can be decomposed as:

$$\mathcal{L} = \mathcal{L}_s + \mathcal{L}_{YM} + \mathcal{L}_f + \mathcal{L}_Y. \quad (1)$$

The scalar Lagrangian is:

$$\mathcal{L}_s = (D^\mu H)^\dagger D_\mu H + (D^\mu \chi)^\dagger D_\mu \chi - V(H, \chi), \quad (2)$$

with the scalar potential given by

$$\begin{aligned} V(H, \chi) &= m^2 H^\dagger H + \mu^2 |\chi|^2 + \begin{pmatrix} H^\dagger H & |\chi|^2 \end{pmatrix} \begin{pmatrix} \lambda_1 & \frac{\lambda_3}{2} \\ \frac{\lambda_3}{2} & \lambda_2 \end{pmatrix} \begin{pmatrix} H^\dagger H \\ |\chi|^2 \end{pmatrix} \\ &= m^2 H^\dagger H + \mu^2 |\chi|^2 + \lambda_1 (H^\dagger H)^2 + \lambda_2 |\chi|^4 + \lambda_3 H^\dagger H |\chi|^2, \end{aligned} \quad (3)$$

where H and χ are the complex scalar Higgs doublet and singlet fields, respectively.

We generalise the *SM* discussion of spontaneous *EW**SB* to the more complicated classical potential of eq. (3). To determine the condition for $V(H, \chi)$ to be bounded from below, it is sufficient to study its behaviour for large field values, controlled by the matrix in the first line of eq. (3). Requiring such a matrix to be positive-definite, we obtain the conditions:

$$4\lambda_1\lambda_2 - \lambda_3^2 > 0, \quad (4)$$

$$\lambda_1, \lambda_2 > 0. \quad (5)$$

If the above conditions are satisfied, we can proceed to the minimisation of V as a function of constant VEVs for the two Higgs fields. Making use of gauge invariance, it is not restrictive to assume:

$$\langle H \rangle \equiv \begin{pmatrix} 0 \\ \frac{v}{\sqrt{2}} \end{pmatrix}, \quad \langle \chi \rangle \equiv \frac{x}{\sqrt{2}}, \quad (6)$$

with v and x real and non-negative. The physically most interesting solutions to the minimisation of eq. (3) are obtained for v and x both non-vanishing:

$$v^2 = \frac{-\lambda_2 m^2 + \frac{\lambda_3}{2} \mu^2}{\lambda_1 \lambda_2 - \frac{\lambda_3^2}{4}}, \quad (7)$$

$$x^2 = \frac{-\lambda_1 \mu^2 + \frac{\lambda_3}{2} m^2}{\lambda_1 \lambda_2 - \frac{\lambda_3^2}{4}}. \quad (8)$$

To compute the scalar masses, we must expand the potential in eq. (3) around the minima in eqs. (7) and (8). We denote by h_1 and h_2 the scalar fields of definite masses, m_{h_1} and

m_{h_2} respectively, and we conventionally choose $m_{h_1}^2 < m_{h_2}^2$. After standard manipulations, the explicit expressions for the scalar mass eigenvalues and eigenvectors are:

$$m_{h_1}^2 = \lambda_1 v^2 + \lambda_2 x^2 - \sqrt{(\lambda_1 v^2 - \lambda_2 x^2)^2 + (\lambda_3 x v)^2}, \quad (9)$$

$$m_{h_2}^2 = \lambda_1 v^2 + \lambda_2 x^2 + \sqrt{(\lambda_1 v^2 - \lambda_2 x^2)^2 + (\lambda_3 x v)^2}, \quad (10)$$

$$\begin{pmatrix} h_1 \\ h_2 \end{pmatrix} = \begin{pmatrix} \cos \alpha & -\sin \alpha \\ \sin \alpha & \cos \alpha \end{pmatrix} \begin{pmatrix} h \\ h' \end{pmatrix}, \quad (11)$$

where $-\frac{\pi}{2} \leq \alpha \leq \frac{\pi}{2}$ fulfils ¹:

$$\sin 2\alpha = \frac{\lambda_3 x v}{\sqrt{(\lambda_1 v^2 - \lambda_2 x^2)^2 + (\lambda_3 x v)^2}}, \quad (12)$$

$$\cos 2\alpha = \frac{\lambda_1 v^2 - \lambda_2 x^2}{\sqrt{(\lambda_1 v^2 - \lambda_2 x^2)^2 + (\lambda_3 x v)^2}}. \quad (13)$$

For our numerical study of the extended Higgs sector, it is useful to invert eqs. (9), (10) and (12), to extract the parameters in the Lagrangian in terms of the physical quantities m_{h_1} , m_{h_2} and $\sin 2\alpha$:

$$\begin{aligned} \lambda_1 &= \frac{m_{h_2}^2}{4v^2}(1 - \cos 2\alpha) + \frac{m_{h_1}^2}{4v^2}(1 + \cos 2\alpha), \\ \lambda_2 &= \frac{m_{h_1}^2}{4x^2}(1 - \cos 2\alpha) + \frac{m_{h_2}^2}{4x^2}(1 + \cos 2\alpha), \\ \lambda_3 &= \sin 2\alpha \left(\frac{m_{h_2}^2 - m_{h_1}^2}{2xv} \right). \end{aligned} \quad (14)$$

Moving to the Yang-Mills Lagrangian \mathcal{L}_{YM} , the non-Abelian field strengths therein are the same as in the *SM* whereas the Abelian ones can be written as follows:

$$\mathcal{L}_{YM}^{\text{Abel}} = -\frac{1}{4}F^{\mu\nu}F_{\mu\nu} - \frac{1}{4}F'^{\mu\nu}F'_{\mu\nu}, \quad (15)$$

where

$$F_{\mu\nu} = \partial_\mu B_\nu - \partial_\nu B_\mu, \quad (16)$$

$$F'_{\mu\nu} = \partial_\mu B'_\nu - \partial_\nu B'_\mu. \quad (17)$$

In this field basis, the covariant derivative is:

$$D_\mu \equiv \partial_\mu + ig_S T^\alpha G_\mu^\alpha + ig T^a W_\mu^a + ig_1 Y B_\mu + i(\tilde{g}Y + g'_1 Y_{B-L})B'_\mu. \quad (18)$$

¹ In all generality, the whole interval $0 \leq \alpha < 2\pi$ is halved because an orthogonal transformation is invariant under $\alpha \rightarrow \alpha + \pi$. We could re-halve the interval by noting that it is invariant also under $\alpha \rightarrow -\alpha$ if we permit the eigenvalues inversion, but this is forbidden by our convention $m_{h_1}^2 < m_{h_2}^2$. Thus α and $-\alpha$ are independent solutions.

The “pure” or “minimal” $B - L$ model is defined by the condition $\tilde{g} = 0$, that implies no mixing between the $B - L$ Z' and SM Z gauge bosons.

The fermionic Lagrangian (where k is the generation index) is given by

$$\begin{aligned} \mathcal{L}_f = \sum_{k=1}^3 & \left(i\overline{q_{kL}}\gamma_\mu D^\mu q_{kL} + i\overline{u_{kR}}\gamma_\mu D^\mu u_{kR} + i\overline{d_{kR}}\gamma_\mu D^\mu d_{kR} + \right. \\ & \left. + i\overline{l_{kL}}\gamma_\mu D^\mu l_{kL} + i\overline{e_{kR}}\gamma_\mu D^\mu e_{kR} + i\overline{\nu_{kR}}\gamma_\mu D^\mu \nu_{kR} \right), \end{aligned} \quad (19)$$

where the fields' charges are the usual SM and $B - L$ ones (in particular, $B - L = 1/3$ for quarks and -1 for leptons with no distinction between generations, hence ensuring universality). The $B - L$ charge assignments of the fields as well as the introduction of new fermionic right-handed heavy neutrinos (ν_R 's) and a scalar Higgs field (χ , with charge $+2$ under $B - L$) are generally designed to ensure the gauge invariance of the theory. Moreover, as we have already mentioned in section I, the heavy neutrinos have also the aim of eliminating the triangular $B - L$ gauge anomalies. Therefore, a $B - L$ gauge extension of the SM gauge group broken at the TeV scale requires at least one new scalar field and three new fermionic fields which are charged with respect to the $B - L$ group.

Finally, the Yukawa interactions are:

$$\begin{aligned} \mathcal{L}_Y = & -y_{jk}^d \overline{q_{jL}} d_{kR} H - y_{jk}^u \overline{q_{jL}} u_{kR} \tilde{H} - y_{jk}^e \overline{l_{jL}} e_{kR} H \\ & - y_{jk}^\nu \overline{l_{jL}} \nu_{kR} \tilde{H} - y_{jk}^M (\overline{\nu_R})_j^\dagger \nu_{kR} \chi + \text{h.c.}, \end{aligned} \quad (20)$$

where $\tilde{H} = i\sigma^2 H^*$ and i, j, k take the values 1 to 3, where the last term is the Majorana contribution and the others the usual Dirac ones.

Neutrino mass eigenstates, obtained after applying the see-saw mechanism, will be called ν_l (with l standing for light) and ν_h (with h standing for heavy), where the first ones are the SM -like ones. With a reasonable choice of Yukawa couplings, the heavy neutrinos can have masses $m_{\nu_h} \sim \mathcal{O}(100)$ GeV.

III. ANALYSIS DETAILS

As spelled out already, the independent physical parameters of the Higgs sector of the scenario considered here are

- m_{h_1} , m_{h_2} and α , the Higgs boson masses and mixing angle. We will span over continuous intervals in the case of the first two quantities while adopting discrete values for

the third one. Masses and couplings (which depend on the Higgs mixing) have been tested against the experimental limits obtained at the Large Electron-Positron (LEP) collider and at the Tevatron.

In order to explore efficiently the expanse of parameter space pertaining to the minimal $B-L$ model, we introduce two extreme conditions, which makes the model intuitive, though at the end it should be borne in mind that intermediate solutions are most probable. The two conditions are obtained by setting:

1. $\alpha = 0$, this is the decoupling limit, with h_1 behaving like the SM Higgs.
2. $\alpha = \frac{\pi}{2}$, which is the so-called inversion limit, in which h_2 is the SM Higgs (though recall that this possibility is phenomenologically not viable, see [26] for a complete analysis in the Higgs singlet extension context).

Furthermore, concerning the strength of Higgs interactions, some of the salient phenomenological behaviours can be summarised as follows:

- SM -like interactions scale with $\cos \alpha (\sin \alpha)$ for $h_1(h_2)$;
- those involving the other new $B-L$ fields, like Z' and heavy neutrinos, scale with the complementary angle, i.e., with $\sin \alpha (\cos \alpha)$ for $h_1(h_2)$;
- triple (and quadruple) Higgs couplings are possible and can induce resonant behaviours, so that, e.g., the $h_2 \rightarrow h_1 h_1$ decay can become dominant if $m_{h_2} > 2m_{h_1}$.

Other than m_{h_1} , m_{h_2} and α , additional parameters are the following.

- g'_1 , the new $U(1)_{B-L}$ gauge coupling. We will adopt discrete perturbative values for this quantity.
- $M_{Z'}$, the new gauge boson mass. An indirect constraint on $M_{Z'}$ comes from analyses at LEP of precision EW data (see [27], based on the analysis of experimental data published in [28–32])²:

$$\frac{M_{Z'}}{g'_1} \geq 7 \text{ TeV} . \quad (21)$$

² A less conservative approach, based on Fermi-type effective four-fermions interactions, gives the weaker constraint $\frac{M_{Z'}}{g'_1} \geq 6 \text{ TeV}$ [33].

Further limits have been obtained at Tevatron [16, 34, 35]. Both have been taken into account here.

- m_{ν_h} , the heavy neutrino masses. We take them to be degenerate and relatively light.
- m_{ν_l} , the SM (or light) neutrino masses. We use the cosmological upper bound $\sum_l m_{\nu_l} < 1$ eV [36]. Ultimately, they have been taken to be $m_{\nu_l} = 10^{-2}$ eV.

(For illustrative purposes we take all neutrino masses, both light and heavy, to be degenerate.)

Notice that the theoretical limits from vacuum stability, triviality and perturbative unitarity obtained in Refs. [23–25] were all taken into account here.

In this paper we will consider only the qualitative results of the analysis of the EW precision constraints made in [26] in the context of singlet scalar extensions of the SM (we assume that the inversion limit is not phenomenologically allowed), though we would like to mention here the fact that in our model, due to the different particle content, the constraints on the precision parameters can be significantly altered (because of, e.g., the presence of heavy neutrinos and the Z' gauge boson in the definition of the EW precision parameters). In the following, we will not investigate these aspects any further.

The numerical analysis was performed with CalcHEP [37] with the model introduced through LanHEP [38]. This implementation was described at length in Ref. [12], so we refer the reader to that publication. A version of the model somewhat improved with respect to the one discussed in Ref. [12] has been used for this work though. Here are the differences.

- The one-loop vertices $g-g-h_1(h_2)$, $\gamma-\gamma-h_1(h_2)$ and $\gamma-Z(Z')-h_1(h_2)$ via W gauge bosons and heavy quarks (top, bottom and charm) have been implemented, adapting the formulae in Ref [39].
- Running masses for top, bottom and charm quarks, evaluated at the Higgs boson mass: $Q = m_{h_1}(m_{h_2})$, depending on which scalar boson is involved in the interaction.
- Running of the QCD coupling constant, at two-loops with 5 active flavours.

Finally, the NLO QCD k -factor for the gluon fusion process [1, 40, 41]³ has been used. Regarding the other processes, we decided to not implement their k -factors since they are

³ Notice that in Ref. [41] (Ref. [1]), $m_t = 174(178)$ GeV, while we used $m_t = 172.5$ GeV as top-quark pole mass value.

much smaller in comparison.

IV. RESULTS

In this section we present our results for the scalar sector of the $B - L$ model. We first present cross-sections at $\sqrt{s} = 7$ and 14 TeV for the two Higgs bosons, as well as their BRs, for some fixed values of the scalar mixing angle α . Its values have been chosen in each plot to highlight some relevant phenomenological aspects. We will then focus on some phenomenologically viable signatures.

A. Standard production mechanisms

In figure 1 we present the cross-sections for the most relevant production mechanisms, i.e., the usual SM processes such as gluon-gluon fusion, vector-boson fusion, $t\bar{t}$ associated production and Higgs-strahlung. For reference, we show in dashed lines the SM case (only for h_1), that corresponds to $\alpha = 0$.

Comparing figure 1c to figure 1a, there is a factor two enhancement passing from $\sqrt{s} = 7$ TeV to $\sqrt{s} = 14$ TeV centre-of-mass energy at the LHC.

The cross-sections are a smooth function of the mixing angle α , so as expected every sub-channel has a cross-section that scales with $\cos \alpha$ ($\sin \alpha$), respectively for h_1 (h_2). As a general rule, the cross-section for h_1 at an angle α is equal to that one of h_2 for $\pi/2 - \alpha$. In particular, the maximum cross-section for h_2 (i.e., when $\alpha = \pi/2$) coincides with cross-section of h_1 for $\alpha = 0$.

We notice that these results are in agreement with the ones that have been discussed in [17, 19, 20] in the context of a scalar singlet extension of the SM , having the latter the same Higgs production phenomenology. Moreover, as already showed in [17], also in the minimal $B - L$ context an high value of the mixing angle could lead to important consequences for Higgs boson discovery at the LHC: a sort of rudimental see-saw mechanism could suppress h_1 production below an observable rate at $\sqrt{s} = 7$ TeV and favour just heavy Higgs boson production, with peculiar final states clearly beyond the SM , or even hide the production of both (if no more than 1 fb^{-1} of data is accumulated). Instead, at $\sqrt{s} = 14$ TeV we expect that at least one Higgs boson will be observed, either the light one or the heavy

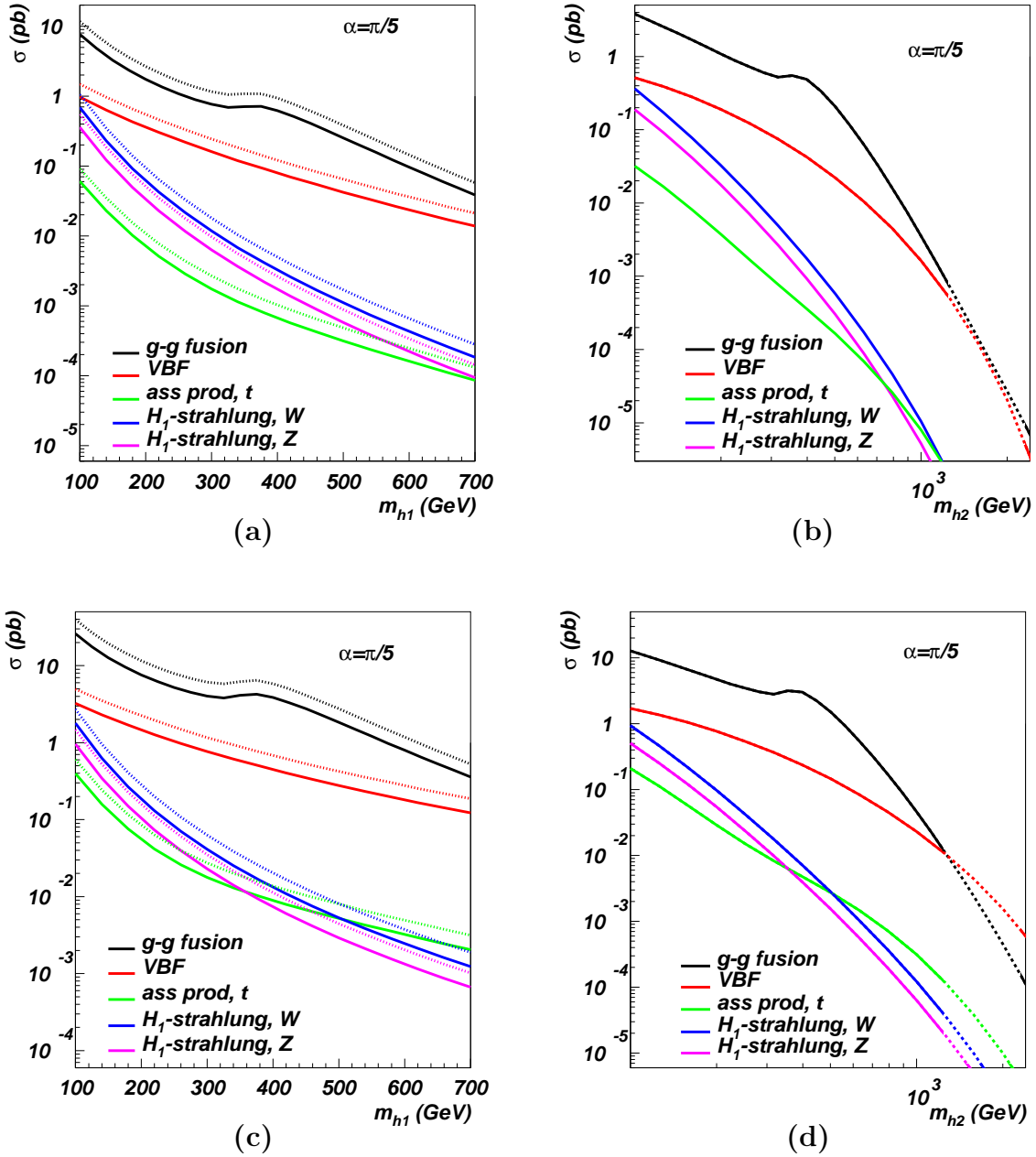


FIG. 1: Cross-sections in the $B - L$ model for h_1 at the LHC (1a) at $\sqrt{s} = 7$ TeV and (1c) at $\sqrt{s} = 14$ TeV, and for h_2 (1b) at $\sqrt{s} = 7$ TeV and (1d) at $\sqrt{s} = 14$ TeV. Dashed lines in figs. (1a) and (1c) refer to $\alpha = 0$. The dotted part of the lines in fig. (1d) refer to h_2 masses excluded by Unitarity (see Ref. [23]).

one, or indeed both, thus shedding light on the scalar sector of the $B - L$ extension of the SM discussed in this work. The region of the parameter space that would allow the scalar sector to be completely hidden, for example for $\alpha \simeq \pi/2$ and m_{h_2} heavy enough to not be

produced, whatever the value of m_{h_1} , is experimentally excluded by precision analyses at LEP [26].

B. Non-standard production mechanisms

All the new particles in the $B-L$ model interact with the scalar sector, so novel production mechanisms can arise considering the exchange of new intermediate particles. Among the new production mechanisms, the associated production of the scalar boson with the Z' boson and the decay of a heavy neutrino into a Higgs boson are certainly the most promising, depending on the specific masses. Notice also that the viable parameter space, that allows a Higgs mass lighter than the SM limit of 114.4 GeV for certain $\alpha - m_{h_2}$ configurations, enables us to investigate also production mechanisms that in the SM are subleading, as the associated production of a Higgs boson with a photon. Figures 2 and 3 show the cross-sections for the non-standard production mechanisms, for $\sqrt{s} = 14$ TeV and several values of α .

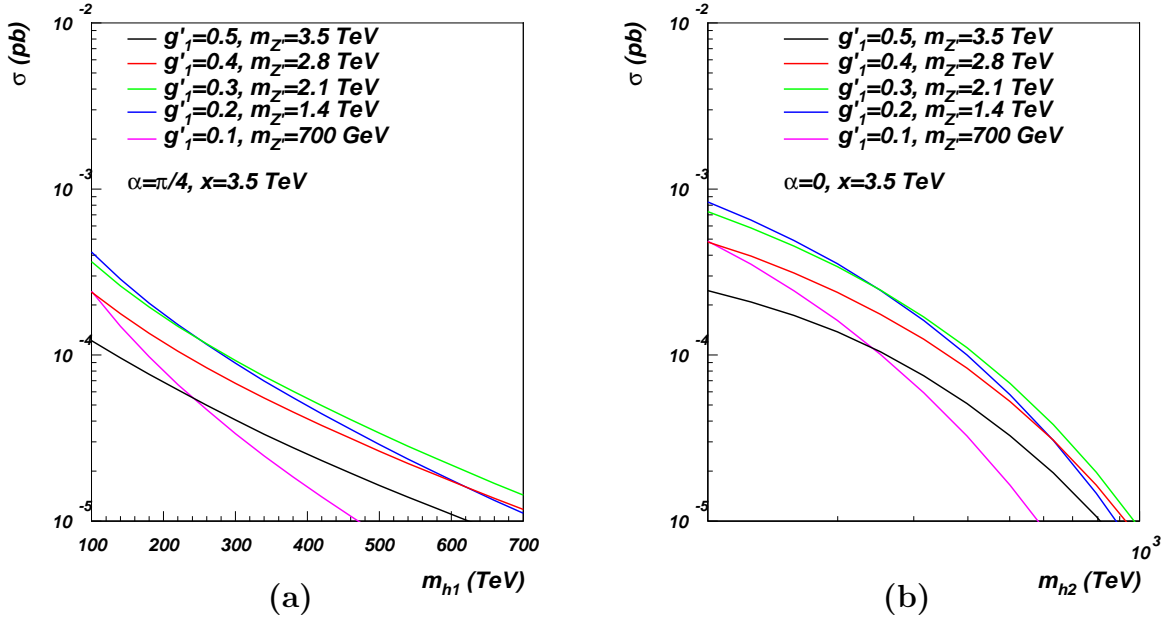


FIG. 2: Cross-sections in the $B-L$ model for the associated production with the Z'_{B-L} boson (2a) of h_1 at $\alpha = \pi/4$ and (2b) of h_2 at $\alpha = 0$.

Figures 2a and 2b show the cross-sections for associated production with the Z' boson of h_1 and of h_2 , respectively, for several combinations of Z' boson masses and g'_1 couplings.

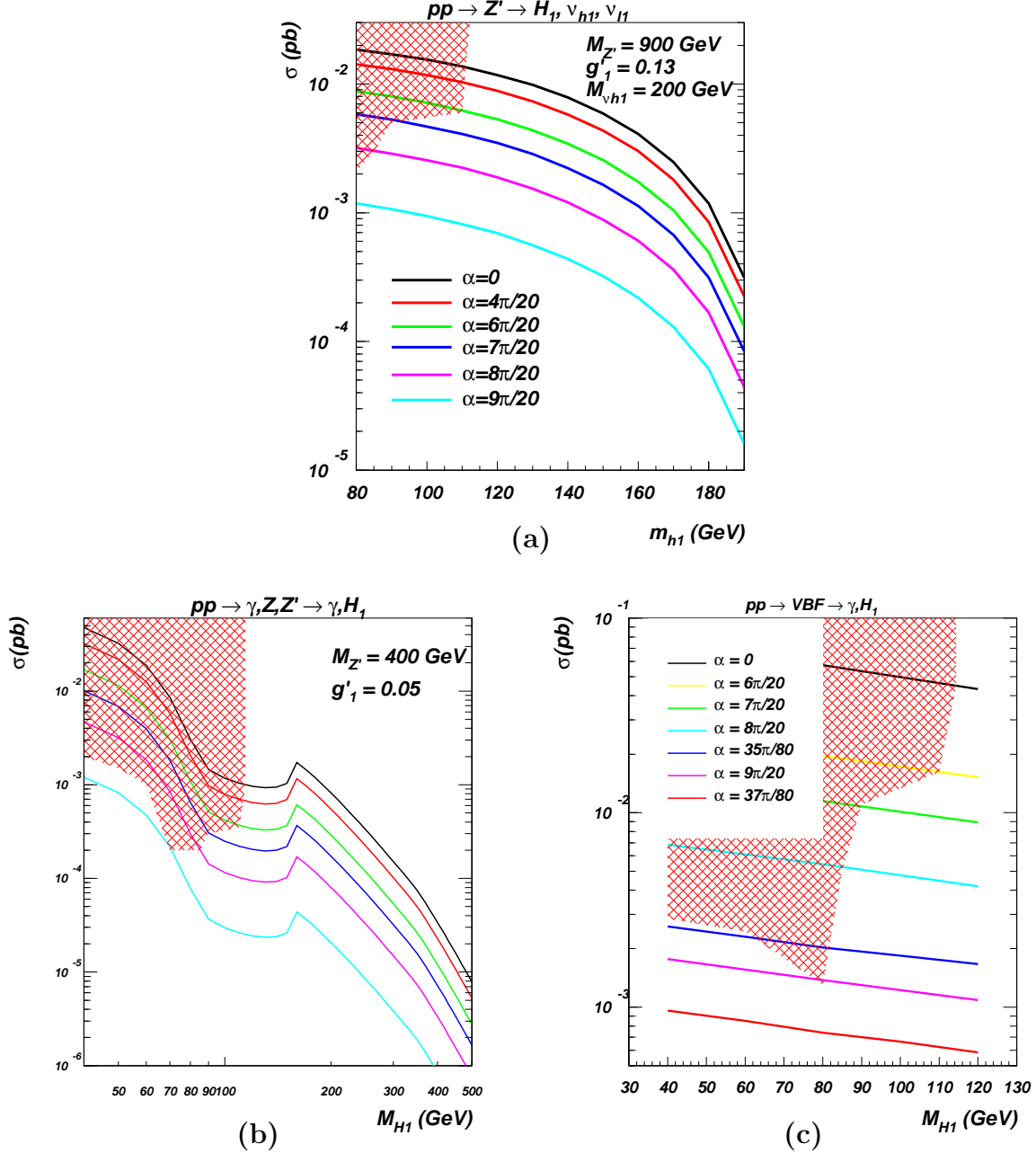


FIG. 3: Cross-sections in the $B - L$ model for the associated production of h_1 (3a) with one heavy and one light neutrinos, (3b) with a photon via γ, Z and Z' bosons exchange (same legend as in fig. (3a) applies here) and (3c) in the vector-boson fusion, all at $\sqrt{s} = 14$ TeV. The red shading is the region excluded by LEP constraints [42].

The process is

$$q \bar{q} \rightarrow Z'^* \rightarrow Z' h_{1(2)}, \quad (22)$$

and it is dominated by the Z' boson's production cross-sections (see [12, 16]). Although

never dominant (always below 1 fb), this channel is the only viable mechanism to produce h_2 in the decoupling scenario, i.e., $\alpha = 0$.

In figure 3 we plot the cross-sections of the other non-standard production mechanisms against the light Higgs mass, for several choices of parameters (as explicitly indicated in the labels). We superimposed the red-shadowed region in order to avoid any value of the cross-section that has been already excluded by LEP constraints (see [42], where the relation between the reduced coupling, in this model, is $\xi^2 = \cos^2 \alpha$), mapping each value of the boundary cross-section as produced by the related maximum value allowed for the light Higgs mass m_{h_1} (at fixed mixing angle α).

First of the showed plots is the decay of a heavy neutrino into a Higgs boson. The whole process chain is

$$q \bar{q} \rightarrow Z' \rightarrow \nu_h \nu_h \rightarrow \nu_h \nu_l h_{1(2)}, \quad (23)$$

and it requires to pair produce heavy neutrinos, again via the Z' boson (see [12, 43] for a detailed analysis of the $pp \rightarrow Z' \rightarrow \nu_h \nu_h$ process and other aspects of Z' and heavy neutrinos phenomenology in the minimal $B-L$ model). Although rather involved, this mechanism has the advantage that the whole decay chain can be of on-shell particles, besides the peculiar final state of a Higgs boson and a heavy neutrino. For a choice of the parameters that roughly maximises this mechanism ($M_{Z'} = 900$ GeV, $g'_1 = 0.13$ and $m_{\nu_h} = 200$ GeV), figure 3a shows that the cross-sections for the production of the light Higgs boson (when only one generation of heavy neutrinos is considered) are above 10 fb for $m_{h_1} < 130$ GeV (and small values of α), dropping steeply when the light Higgs boson mass approaches the kinematical limit for the heavy neutrino to decay into it. Assuming the transformation $\alpha \rightarrow \pi/2 - \alpha$, the production of the heavy Higgs boson via this mechanism shows analogous features.

Next, figures 3b and 3c shows the associated production of the light Higgs boson with a photon. The processes are, respectively,

$$q \bar{q} \rightarrow \gamma/Z/Z' \rightarrow \gamma h_1 \quad (24)$$

via the SM neutral gauge bosons (γ and Z) and the new Z' boson, and

$$q q' \rightarrow \gamma h_1 q'' q''' , \quad (25)$$

through vector-boson fusion (only W and Z bosons).

In the first instance, we notice that the Z' sub-channel in eq. (24) is always negligible, as there is no $Z' - W - W$ interaction and the $V - h - \gamma$ effective vertex is only via a top quark loop (an order of magnitude lower than the $V - h - \gamma$ effective vertex via a W boson loop) [39]. What is relevant in these two channels is that the light Higgs boson mass can be considerably smaller than the LEP limit (they are valid for the SM , or equivalently when $\alpha = 0$ in the $B - L$ model). Hence, the phase space factor can enhance the mechanism of eq. (24) for small masses, up to the level of 1 fb for $m_{h_1} < 60$ GeV (and suitable values of the mixing angle α , depending on the experimental and theoretical limits, see Refs. [23, 24] for a complete treatment of the allowed parameter space of the Higgs sector of the minimal $B - L$ problem). Moreover, it has recently been observed that the associated production with a photon in the vector-boson fusion channel could be useful for low Higgs boson masses to trigger events in which the Higgs boson decays into b -quark pairs [44]. Complementary to that, the process in eq. (24) can also be of similar interest, with the advantage that the photon will always be back-to-back relative to the b -quark pair. For comparison, figures 3b and 3c show the cross-section for these processes⁴. Certainly, for a h_1 boson heavier than the SM limit, vector-boson fusion is the dominant process for associated production of h_1 with a photon, and this is also true for $m_{h_1} > 60$ GeV. However, for light Higgs boson masses lower than 60 GeV, the two mechanisms of eqs. (24) and (25) become equally competitive, up to the level of $\mathcal{O}(1)$ fb each, for suitable values of the mixing angle α .

C. Branching ratios and total widths

Moving to the Higgs boson decays, figure 4 shows the BRs for both the Higgs bosons, h_1 and h_2 , respectively. Only the two-body decay channels are shown here.

Regarding the light Higgs boson, the only new particle it can decay into is the heavy neutrino (we consider a very light Z' boson unlikely and unnatural), if the channel is kinematically open. In figure 4a we show this case, for a small heavy neutrino mass, i.e., $m_{\nu_h} = 50$ GeV, and we see that the relative BR of this channel can be rather important, as the decay into b -quark pairs or into W boson pairs, in the range of masses $110 \text{ GeV} \leq m_{h_1} \leq 150 \text{ GeV}$. Such range happens to be critical in the SM since here the SM Higgs boson passes

⁴ In order to produce figure 3c, we included the following cuts: $P_t^{\gamma, \text{jet}} > 15 \text{ GeV}$, $|\eta^\gamma| < 3$ and $|\eta^{\text{jet}}| < 5.5$, where “jet” refers to the actual final state, though we use partons here to emulate it [44].

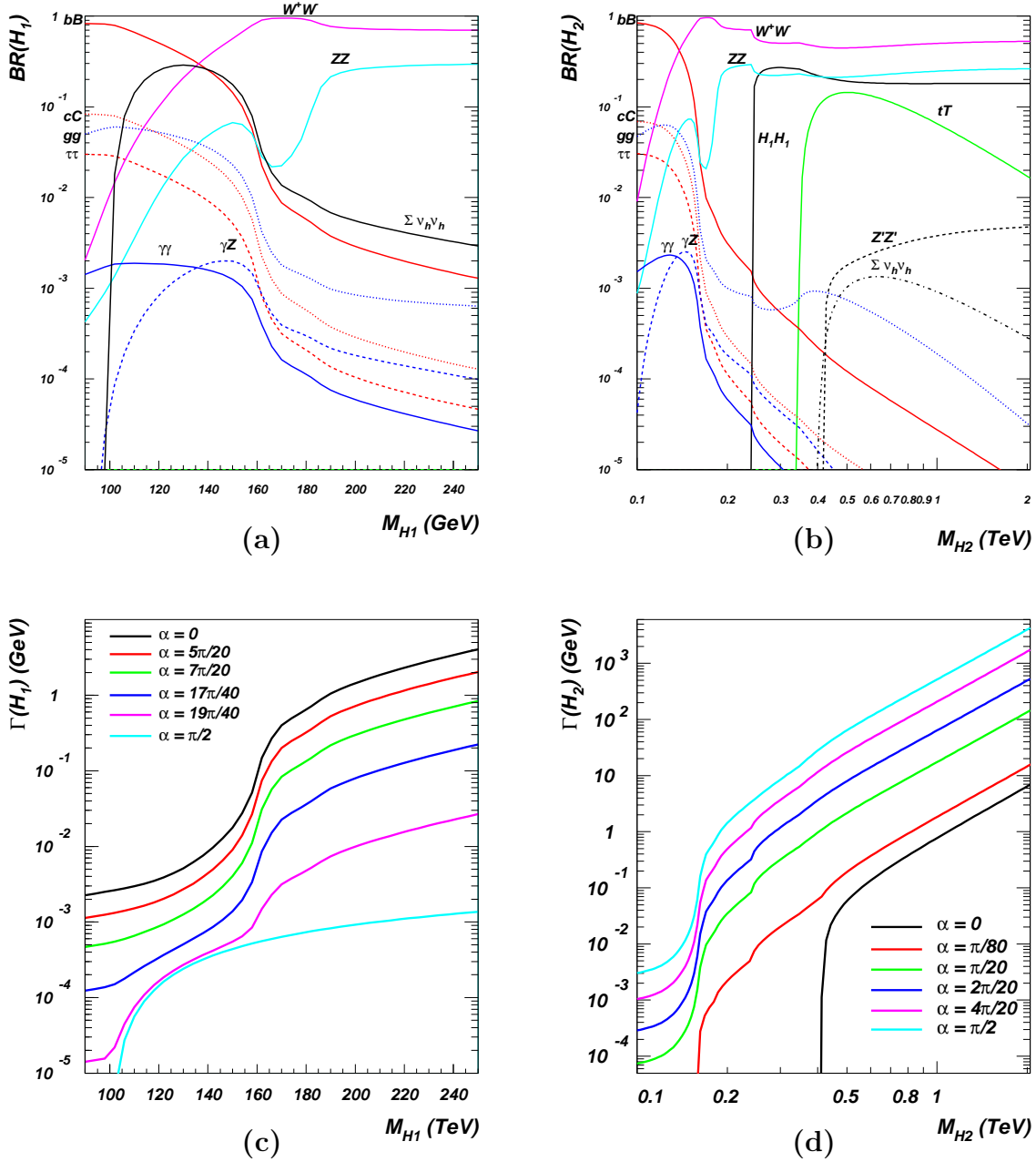


FIG. 4: (4a) Branching ratios for h_1 for $\alpha = 2\pi/5$ and $m_{\nu_h} = 50$ GeV and (4c) h_1 total width for a choice of mixing angles and (4b) BRs for h_2 for $\alpha = 3\pi/20$ and $m_{h_1} = 120$ GeV, $M_{Z'} = 210$ GeV and $m_{\nu_h} = 200$ GeV and (4d) h_2 total width for a choice of mixing angles.

from decaying dominantly into b -quark pairs to a region in masses in which the decay into W boson pairs is the prevailing one. These two decay channels have completely different signatures and discovery methods/powers. The fact that the signal of the Higgs boson de-

caying into b -quark pairs is many orders of magnitude below the natural QCD background, spoils its sensitivity. In the case of the $B - L$ model, the decay into heavy neutrino pairs is therefore phenomenologically very important, besides being an interesting feature of the $B - L$ model if $m_{\nu_h} < M_W$, as it allows multileptons signatures of the light Higgs boson. Among them, there is the decay of the Higgs boson into 3ℓ , $2j$ and \cancel{E}_T (that we have already studied for the Z' case in Ref.[12] and that will be reported upon separately for the Higgs boson case [45]), into 4ℓ and \cancel{E}_T (as, again, already studied for the Z' case in Ref. [14]) or into 4ℓ and $2j$ (as already studied, when $\ell = \mu$, in the 4^{th} family extension of the SM [46]). All these peculiar signatures allow the Higgs boson signal to be studied in channels much cleaner than the decay into b -quark pairs.

In the case of the heavy Higgs boson, further decay channels are possible in the $B - L$ model, if kinematically open. The heavy Higgs boson can decay in pairs of the light Higgs boson ($h_2 \rightarrow h_1 h_1$) or even in triplets ($h_2 \rightarrow h_1 h_1 h_1$), in pairs of heavy neutrinos and Z' bosons. Even for a small value of the angle, figure 4b shows that the decay of a heavy Higgs boson into pairs of the light one can be quite sizeable, at the level of the decay into SM Z bosons for $m_{h_1} = 120$ GeV. It is important to note that this channel does not have a simple dependence on the mixing angle α , as we can see in figure 5.

The BRs of the heavy Higgs boson decaying into Z' boson pairs and heavy neutrino pairs decrease as the mixing angle increases, getting to their maxima (comparable to the W and Z ones) for a vanishing α , for which the production cross-section is however negligible. As usual, and also clear from figure 4b, the decay of the heavy Higgs boson into gauge bosons (the Z' boson) is always bigger than the decay into pairs of fermions (the heavy neutrinos, even when summed over the generations as plotted), when they have comparable masses (here, $M_{Z'} = 210$ GeV and $m_{\nu_h} = 200$ GeV).

The other standard decays of both the light and the heavy Higgs bosons are not modified substantially in the $B - L$ model (i.e., the Higgs boson to W boson pairs is always dominant when kinematically open, while before that the decay into b -quarks is the prevailing one; further, radiative decays, such as Higgs boson decays into pairs of photons, peak at around 120 GeV, etc.). Only when other new channels open, the standard decay channels alter accordingly. This rather common picture could be altered when the mixing angle α approaches $\pi/2$, but such situation is phenomenologically not viable [26].

Figures 4c and 4d show the total widths for h_1 and h_2 , respectively. In the first case,

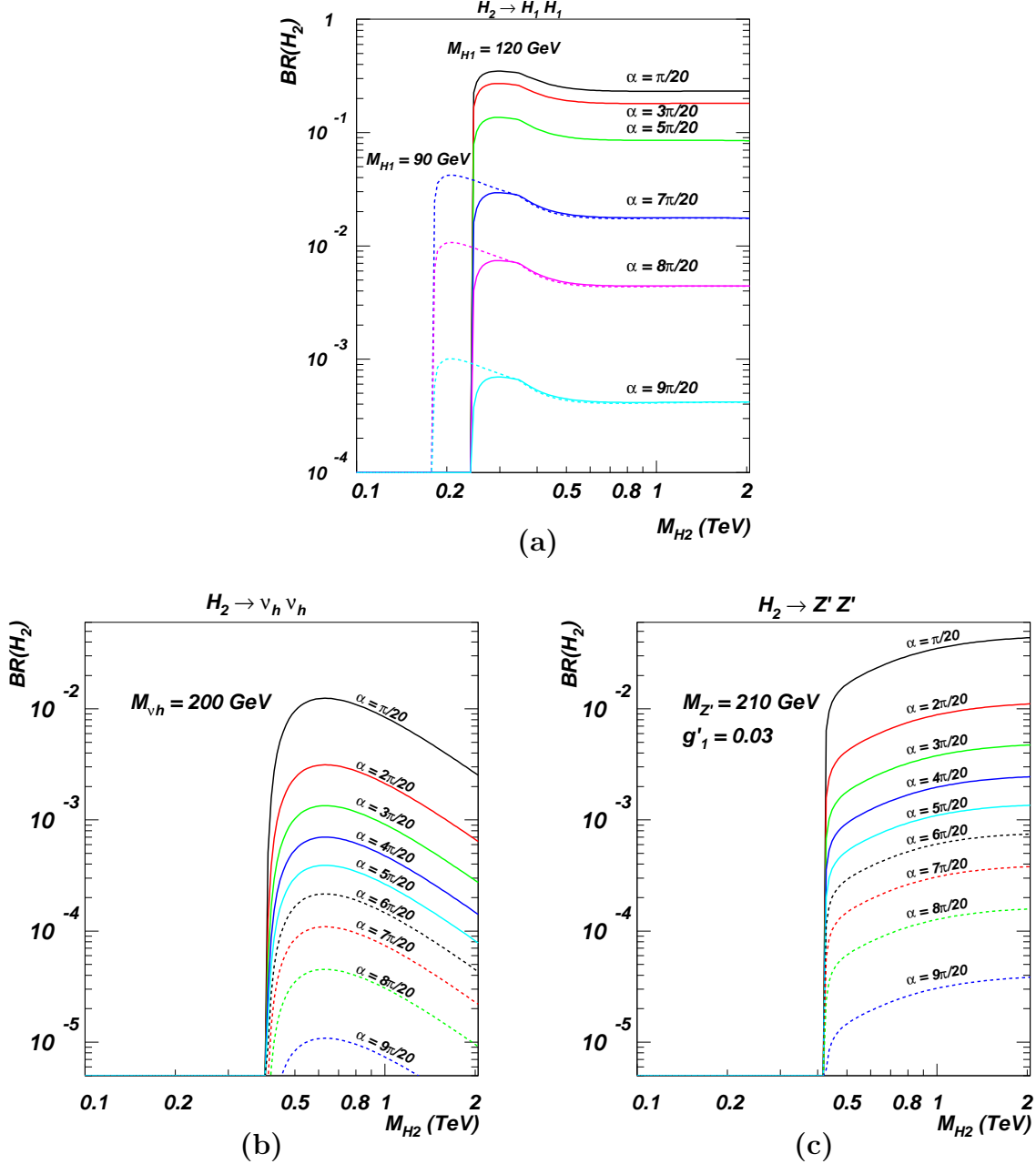


FIG. 5: Dependence on the mixing angle α of (5a) $BR(h_2 \rightarrow h_1 h_1)$, of (5b) $BR(h_2 \rightarrow \nu_h \nu_h)$ and of (5c) $BR(h_2 \rightarrow Z' Z')$.

few thresholds are clearly recognisable, as the heavy neutrino one at 100 GeV (for angles very close to $\pi/2$ only), the W and the Z ones. Over the mass range considered ($90 \text{ GeV} < m_{h_1} < 250 \text{ GeV}$, the particle's width) is very small until the W threshold, less than $1 - 10 \text{ MeV}$, rising steeply to few GeV for higher h_1 masses and small angles (i.e., for a SM -like light Higgs boson). As we increase the mixing angle, the couplings of the light Higgs boson to SM particles is reduced, as so its total width.

On the contrary, as we increase α , the h_2 total width increases, as clear from figure 4d. Also in this case, few thresholds are recognisable, as the usual W and Z gauge boson ones, the light Higgs boson one (at 240 GeV) and the t -quark one (only for big angles, i.e., when h_2 is the SM -like Higgs boson). When the mixing angle is small, the h_2 total width stays below 1 GeV all the way up to $m_{h_2} \sim 300 \div 500$ GeV, rising as the mass increases towards values for which $\Gamma_{h_2} \sim m_{h_2} \sim 1$ TeV and h_2 loses the meaning of resonant state, only for angles very close to $\pi/2$. Instead, if the angle is small, i.e., less than $\pi/10$, the ratio of width over mass is less than 10% and the heavy Higgs boson is a well defined particle. In the decoupling regime, i.e., when $\alpha = 0$, the only particles h_2 couples to are the Z' and the heavy neutrinos. The width is therefore dominated by the decay into them and is tiny, as clear from figure 4d.

As already mentioned, figure 5 shows the dependence on the mixing angle α of the BRs of h_2 into pairs of non- SM particles. In particular, we consider the decays $h_2 \rightarrow h_1 h_1$ (for two different h_1 masses, $m_{h_1} = 90$ GeV and $m_{h_1} = 120$ GeV, only for the allowed values of α), $h_2 \rightarrow \nu_h \nu_h$ and $h_2 \rightarrow Z' Z'$ (not influenced by m_{h_1}). As discussed in section III, the interaction of the heavy Higgs boson with SM (or non- SM) particles has an overall $\sin \alpha$ (or $\cos \alpha$, respectively) dependence. Nonetheless, the BRs in figure 5 depend also on the total width, that for $\alpha > \pi/4$ is dominated by the $h_2 \rightarrow W^+ W^-$ decay. Hence, when the angle assumes big values, the angle dependence of the h_2 BRs into heavy neutrino pairs and into Z' boson pairs follow a simple $\cot \alpha$ behaviour. Regarding $h_2 \rightarrow h_1 h_1$, its BR is complicated by the fact that the contribution of this process to the total width is not negligible when the mixing angle is small, i.e., $\alpha < \pi/4$. In general, this channel vanishes when $\alpha \rightarrow 0$, and it gets to its maximum, of around 10% \div 30% of the total width, as α takes a non-trivial value, being almost constant with the angle if it is small enough.

The heavy Higgs boson can be relatively massive and the tree-level three-body decays are interesting decay modes too. Besides being clear BSM signatures, they are crucial to test the theory behind the observation of any scalar particle: its self-interactions and the quartic interactions with the vector bosons could be tested directly in these decay modes. In the $B - L$ model with no $Z - Z'$ mixing, the quartic interactions that can be tested as h_2 decay modes, if the respective channels are kinematically open, are: $h_2 \rightarrow h_1 h_1 h_1$, $h_2 \rightarrow h_1 W^+ W^-$ and $h_2 \rightarrow h_1 Z Z$, as shown in figure 6, again for $m_{h_1} = 90$ GeV and 120 GeV. Although possible, $h_2 \rightarrow h_1 Z' Z'$ is negligible always, even if the Z' boson is light

enough to allow the decay. For $M_{Z'} = 210$ GeV, $\text{BR}(h_2 \rightarrow h_1 Z' Z') \lesssim 10^{-5}$ for $m_{h_2} < 2$ TeV.

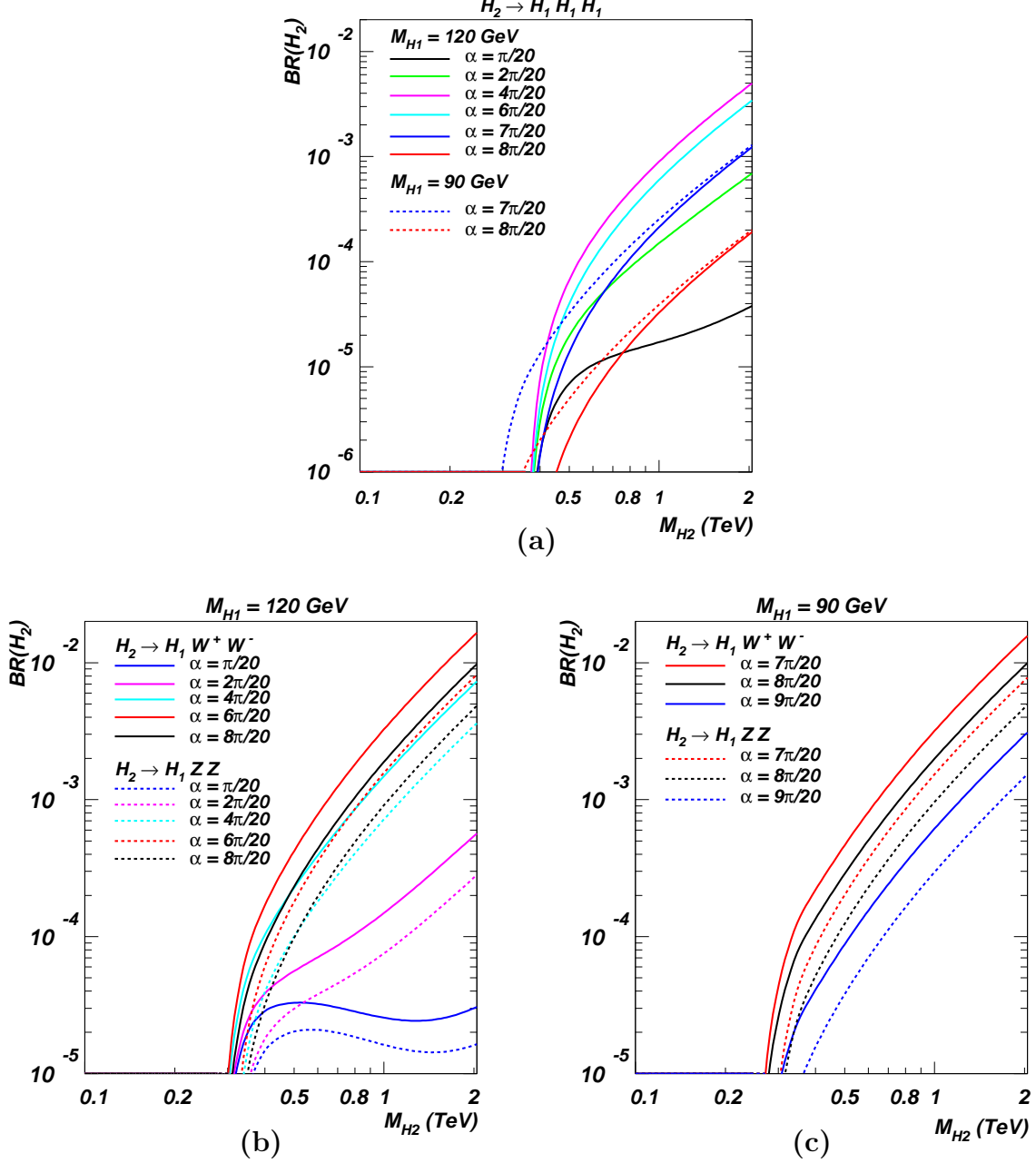


FIG. 6: Dependence on the mixing angle α of the three body decays (6a) $\text{BR}(h_2 \rightarrow h_1 h_1 h_1)$ and (6b) $\text{BR}(h_2 \rightarrow h_1 V V)$ ($V = W^\pm, Z$) for $m_{h_1} = 120$ GeV and (6c) for $m_{h_1} = 90$ GeV, respectively.

The BRs for both the $h_2 \rightarrow h_1 h_1 h_1$ and the $h_2 \rightarrow h_1 V V$ ($V = W^\pm, Z$) channels are maximised roughly when the mixing between the two scalars is maximum, i.e., when $\alpha \sim \pi/4$, regardless of m_{h_1} . The former channel, that is interesting because would produce

three light Higgs bosons simultaneously, can contribute at most at 10^{-3} of the total width for h_2 , as we are neglecting values of m_{h_2} and α for which $\Gamma_{h_2} \sim m_{h_2}$ (see figure 4d). For instance, for $m_{h_2} = 800$ GeV, α needs to be less than $\pi/5$ to have a reasonable small width-over-mass ratio ($\sim 10\%$), and $\text{BR}(h_2 \rightarrow h_1 h_1 h_1) \leq 0.6 \cdot 10^{-3}$. The situation is similar for the latter channel, involving pairs of *SM* gauge bosons. Again, for $m_{h_2} = 800$ GeV and $\alpha = \pi/5$, $\text{BR}(h_2 \rightarrow h_1 W^+ W^-) = 2 \text{BR}(h_2 \rightarrow h_1 Z Z) = 10^{-3}$ for $m_{h_1} = 120$ GeV. For $m_{h_1} = 90$ GeV, the mixing angle is constrained to be bigger than $7\pi/20$. For these values and the same m_{h_2} as before, such BRs are doubled.

D. Event Rates

In this section we combine the results from the Higgs boson cross-sections and those from the BR analysis in order to perform a detailed study of typical event rates for some Higgs signatures which are specific to the $B - L$ model.

Before all else, it is important to identify two different experimental scenarios related to the LHC: we will generally refer to an “early discovery scenario” by considering an energy in the hadronic Centre-of-Mass (CM) of $\sqrt{s} = 7$ TeV and an integrated luminosity of $\int L = 1 \text{ fb}^{-1}$ (according to the official schedule, this is what is expected to be collected after the first couple of years of LHC running) and to a “full luminosity scenario” by considering an energy in the hadronic CM of $\sqrt{s} = 14$ TeV and an integrated luminosity of $\int L = 300 \text{ fb}^{-1}$ (according to the official schedule, this is what is expected to be realistically collected at the higher energy stage).

As we shall see by combining the production cross-sections and the decay BRs presented in the previous subsections, the two different scenarios open different possibilities for the detection of peculiar signatures of the model: in the “early discovery scenario” there is a clear possibility to detect a light Higgs state yielding heavy neutrino pairs while the “full luminosity scenario” affords the possibility of numerous discovery mechanisms (in addition to the previous mechanism, for the heavy Higgs state one also has decays of the latter into Z' boson and light Higgs boson pairs).

Firstly, we focus on the “early discovery scenario”: in this experimental configuration, the most important $B - L$ distinctive process is represented by heavy neutrino pair production via a light Higgs boson, through the channel $pp \rightarrow h_1 \rightarrow \nu_h \nu_h$. In figure 7 we show the

explicit results for the $pp \rightarrow h_1 \rightarrow \nu_h \nu_h$ process at the LHC with $\sqrt{s} = 7$ TeV, for $m_{\nu_h} = 50$ GeV (figure (7a)) and $m_{\nu_h} = 60$ GeV (figure (7b)), obtained by combining the light Higgs boson production cross-section via gluon-gluon fusion only (since it represents the main contribution) and the BR of the light Higgs boson to heavy neutrino pairs. The obtained rate is projected in the m_{h_1} - α plane and several values of the cross-section times BR have been considered: $\sigma = 5, 10, 50, 100$ and 250 fb. The red-shadowed region takes into account the exclusion limits established by the LEP experiments.

Even considering a low-luminosity scenario (i.e., $\int L \simeq 1 \text{ fb}^{-1}$), there is a noticeable allowed parameter space for which the rate of such events is considerably large: in the case of $m_{\nu_h} = 50$ GeV, when the integrated luminosity reaches $\int L = 1 \text{ fb}^{-1}$, we estimated a collection of ~ 10 heavy neutrino pairs from the light Higgs boson production and decay for $100 \text{ GeV} < m_{h_1} < 170 \text{ GeV}$ and $0.05\pi < \alpha < 0.48\pi$, that scales up to $\sim 10^2$ events for $110 \text{ GeV} < m_{h_1} < 155 \text{ GeV}$ and $0.16\pi < \alpha < 0.46\pi$. In the case of $m_{\nu_h} = 60$ GeV, we estimated a collection of ~ 10 heavy neutrino pairs from Higgs production for $120 \text{ GeV} < m_{h_1} < 170 \text{ GeV}$ and $0.06\pi < \alpha < 0.48\pi$, that scales up to $\sim 10^2$ events for $125 \text{ GeV} < m_{h_1} < 150 \text{ GeV}$ and $0.25\pi < \alpha < 0.44\pi$.

If we consider instead the “full luminosity scenario”, there are several important distinctive signatures: $pp \rightarrow h_2 \rightarrow h_1 h_1$, $pp \rightarrow h_2 \rightarrow Z' Z'$ and $pp \rightarrow h_2 \rightarrow \nu_h \nu_h$. In figure 8 we show the results for light Higgs boson pair production from heavy Higgs boson decays at the LHC with $\sqrt{s} = 14$ TeV for $m_{h_1} = 120$ GeV (figure (8a)) and $m_{h_1} = 240$ GeV (figure (8b)). Again, if we project the rates on the bi-dimensional m_{h_2} - α plane, we can select the contours that relate the cross-section times BR to some peculiar values.

Considering an integrated luminosity of 300 fb^{-1} , we can relate $\sigma = 25(250)$ fb to $7500(75000)$ events, hence for both choices of the light Higgs mass the α - m_{h_2} parameter space offers an abundant portion in which the event rate is noticeable for light Higgs boson pair production from heavy Higgs boson decays: when $m_{h_1} = 120$ GeV the process is accessible almost over the entire parameter space, with a cross-section peak of 400 fb in the $240 \text{ GeV} < m_{h_2} < 400 \text{ GeV}$ and $0.13\pi < \alpha < 0.30\pi$ intervals, while in the $m_{h_1} = 240$ GeV case the significant parameter space is still large, even if slightly decreased, with a cross-section peak of 25 fb in the $480 \text{ GeV} < m_{h_2} < 800 \text{ GeV}$ and $0.06\pi < \alpha < 0.32\pi$ region.

In figure 9 we show the results for Z' boson pair production from heavy Higgs boson decays at the LHC with $\sqrt{s} = 14$ TeV for $m_{Z'} = 210$ GeV (figure (9a)) and $m_{Z'} = 280$ GeV (figure

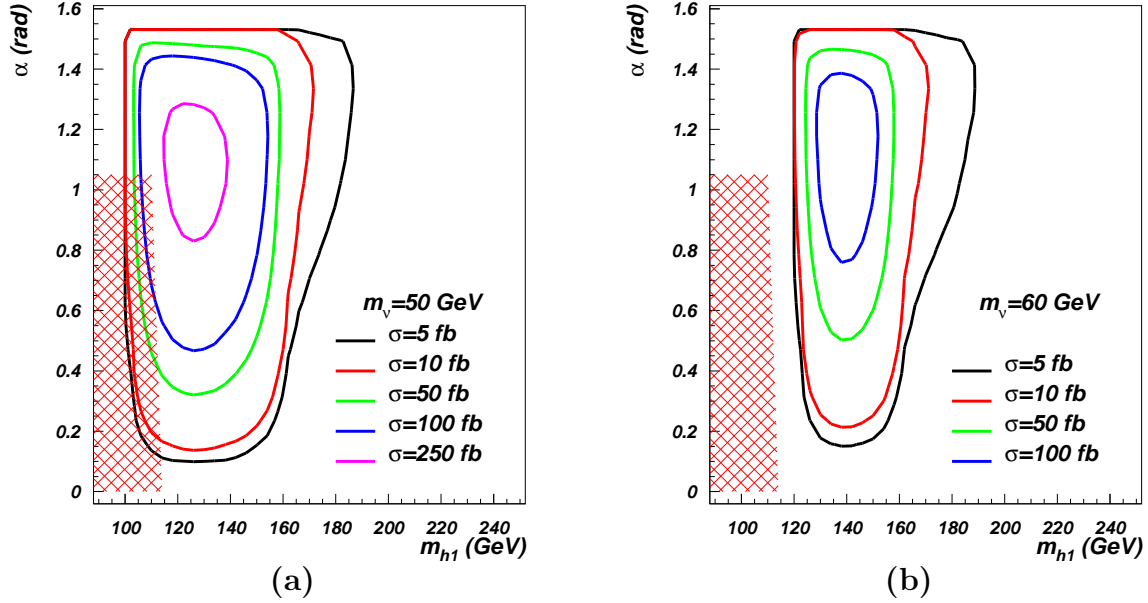


FIG. 7: Cross-section times BR contour plot for the $B - L$ process $pp \rightarrow h_1 \rightarrow \nu_h \nu_h$ at the LHC with $\sqrt{s} = 7$ TeV, plotted against m_{h_1} - α , with $m_{\nu_h} = 50$ GeV (7a) and $m_{\nu_h} = 60$ GeV (7b). Several values of cross-section times BR have been considered: $\sigma = 5$ fb (black line), $\sigma = 10$ fb (red line), $\sigma = 50$ fb (green line), $\sigma = 100$ fb (blue line) and $\sigma = 250$ fb (violet line). The red-shadowed region is excluded by the LEP experiments.

(9b)). Again, if we project the rates on the bi-dimensional m_{h_2} - α plane, we can select the contours that relate the cross-section times BR to some peculiar values. Here, we have that $\sigma = 0.085(0.85)$ fb corresponds to 25(250) events, hence for both choices of Z' mass the α - m_{h_2} parameter space offers an abundant portion in which the event rate could be interesting for Z' boson pair production from heavy Higgs boson decays: for $m_{Z'} = 210$ GeV the process has a peak of 0.85 fb in the $420 \text{ GeV} < m_{h_2} < 650 \text{ GeV}$ and $0.03\pi < \alpha < 0.25\pi$ region, while if $m_{Z'} = 280$ GeV a noticeable parameter space is still potentially accessible with a rate peak of 0.3 fb (100 events) in the $560 \text{ GeV} < m_{h_2} < 800 \text{ GeV}$ and $0.03\pi < \alpha < 0.19\pi$ region.

In analogy with the previous two cases, in figure 10 we show the results for heavy neutrino pair production at the LHC with $\sqrt{s} = 14$ TeV plus $m_{\nu_h} = 150$ GeV (figure (10a)) and $m_{\nu_h} = 200$ GeV (figure (10b)). The usual contour plot displays a sizable event rate in the α - m_{h_2} parameter space for both choices of the ν_h mass. For example, when $m_{\nu_h} = 150$ GeV we find a cross-section times BR peak of 0.85 fb (~ 250 events) in the $320 \text{ GeV} < m_{h_2} < 520 \text{ GeV}$ and $0.03\pi < \alpha < 0.33\pi$ region, while if $m_{\nu_h} = 200$ GeV we find a peak of 0.85 fb in

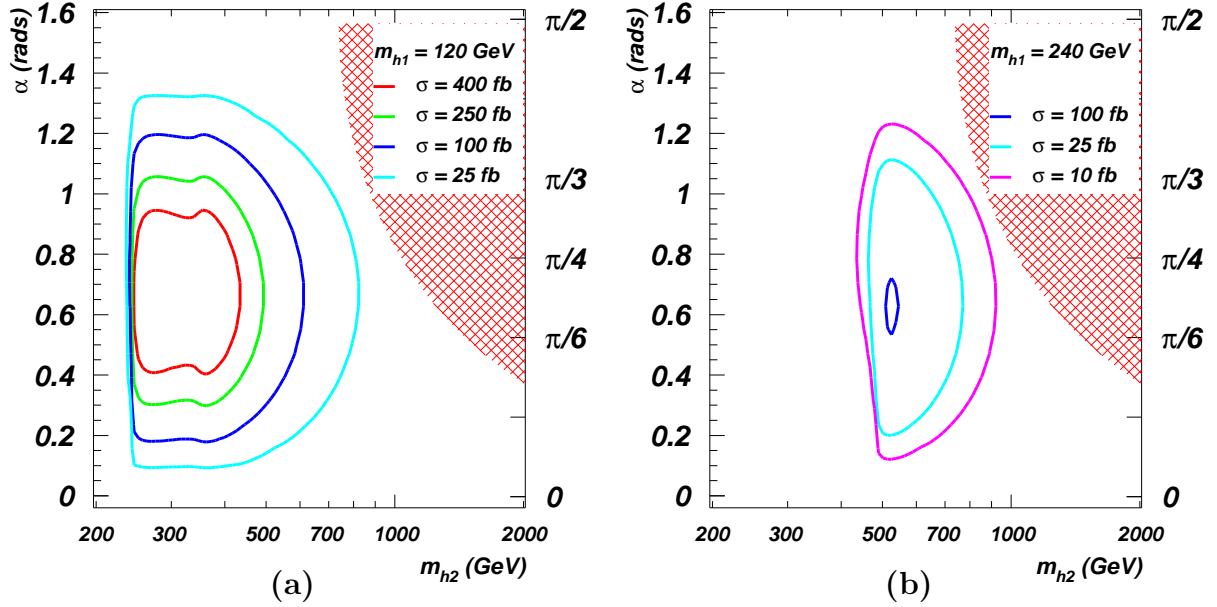


FIG. 8: Cross-section times BR contour plot for the $B - L$ process $pp \rightarrow h_2 \rightarrow h_1 h_1$ at the LHC with $\sqrt{s} = 14$ TeV, plotted against m_{h_2} - α , with $m_{h_1} = 120$ GeV (8a) and $m_{h_1} = 240$ GeV (8b). Several values of cross-section times BR have been considered: $\sigma = 10$ fb (violet line), $\sigma = 25$ fb (light-blue line), $\sigma = 100$ fb (blue line), $\sigma = 250$ fb (green line) and $\sigma = 400$ fb (red line). The red-shadowed region is excluded by unitarity constraints.

the $450 \text{ GeV} < m_{h_2} < 550 \text{ GeV}$ and $0.03\pi < \alpha < 0.21\pi$ region.

V. CONCLUSIONS

In summary, we have studied in detail the Higgs sector of the minimal $B - L$ model at both the foreseen energy stages of the LHC (and corresponding luminosities). While virtually all relevant production and decay processes of the two Higgs states of the model have been investigated, we have eventually paid particular attention to those that are peculiar to the described $B - L$ scenario. The phenomenological analysis has been carried out in presence of all available theoretical and experimental constraints and by exploiting numerical programs at the parton level. While many Higgs signatures already existing in the SM could be replicated in the case of its $B - L$ version, in either of the two Higgs states of the latter (depending on their mixing), it is more important to notice that several novel Higgs processes could act as hallmarks of the minimal $B - L$ model. These include Higgs production via

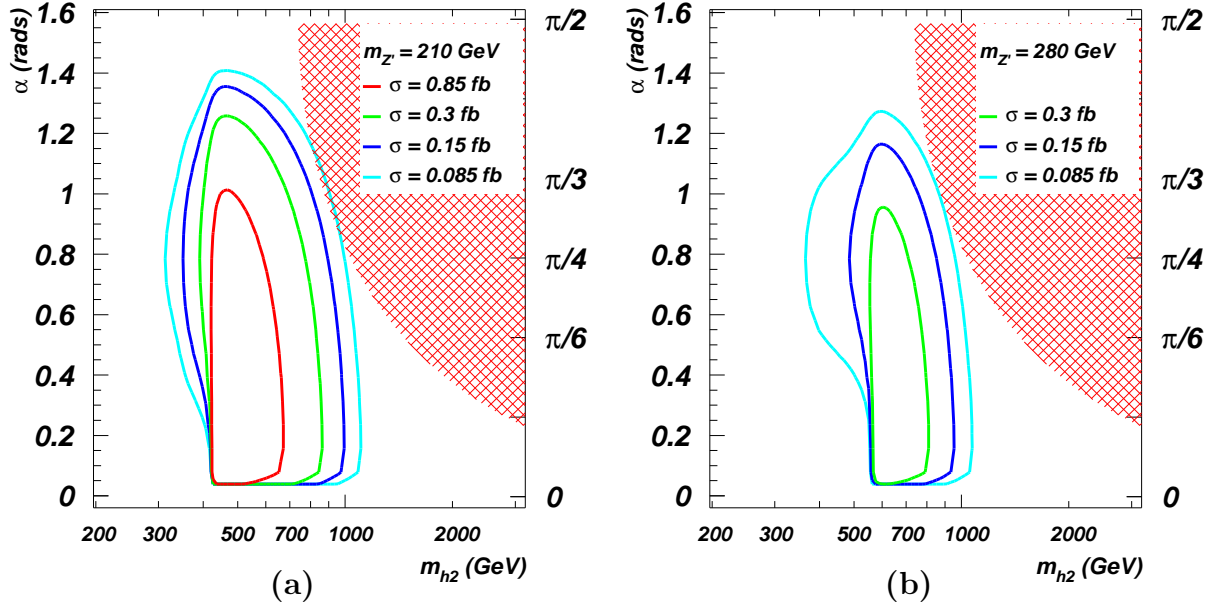


FIG. 9: Cross-section times BR contour plot for the $B - L$ process $pp \rightarrow h_2 \rightarrow Z'Z'$ at the LHC with $\sqrt{s} = 14$ TeV, plotted against m_{h_2} - α , with $m_{Z'} = 210$ GeV (9a) and $m_{Z'} = 280$ GeV (9b). Several values of cross-section times BR have been considered: $\sigma = 0.085$ fb (light-blue line), $\sigma = 0.15$ fb (blue line), $\sigma = 0.3$ fb (green line), $\sigma = 0.85$ fb (red line). The red-shadowed region is excluded by unitarity constraints.

gluon-gluon fusion, in either the light or heavy Higgs state, the former produced at the lower energy stage of the CERN collider and decaying in two heavy neutrinos and the latter produced at the higher energy stage of such a machine and decaying not only in heavy neutrino pairs but also in Z' and light Higgs ones. For each of these signatures we have in fact found parameter space regions where the event rates are sizable and potentially amenable to discovery. While, clearly, detailed signal-to-background analyses will have to either confirm or disprove the possibility of the latter, our results have laid the basis for the phenomenological exploitation of the Higgs sector of the minimal $B - L$ model at the LHC.

ACKNOWLEDGEMENTS

We would like to thank D.A. Ross and C.H. Shepherd-Themistocleous for most useful comments and discussions plus A. Belyaev for the same and for his help in implementing the gg -fusion process and the appropriate Higgs boson widths in CalcHEP as well as for

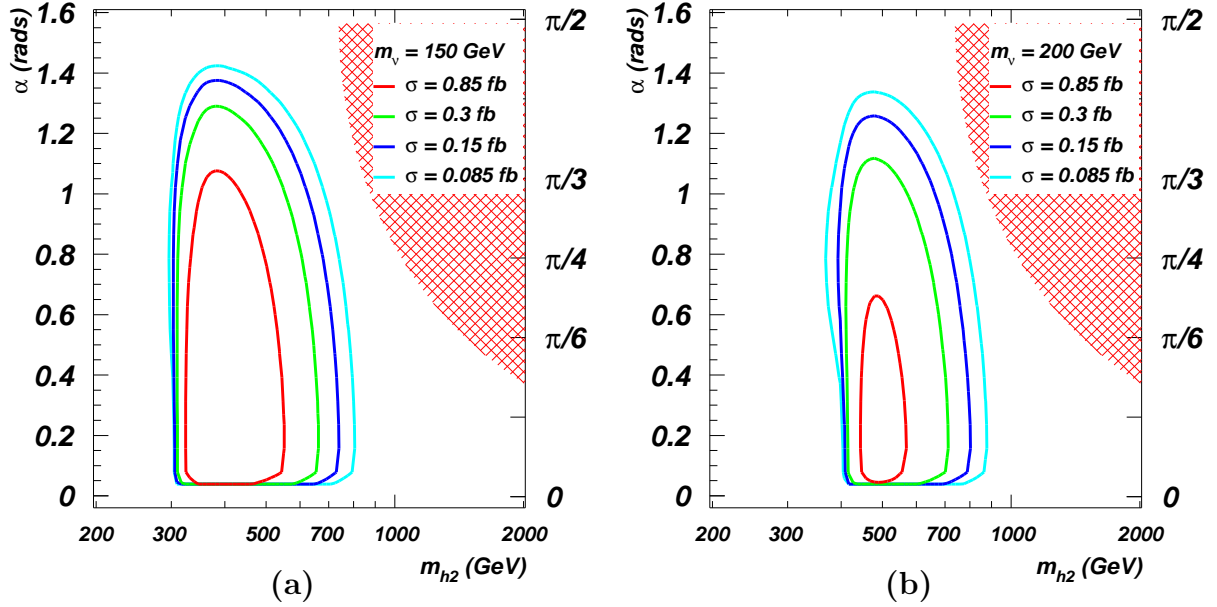


FIG. 10: Cross-section times BR contour plot for the $B-L$ process $pp \rightarrow h_2 \rightarrow \nu_h \nu_h$ at the LHC with $\sqrt{s} = 14$ TeV, plotted against m_{h_2} - α , with $m_{\nu_h} = 150$ GeV (10a) and $m_{\nu_h} = 200$ GeV (10b). Several values of cross-section times BR have been considered: $\sigma = 0.085$ fb (light-blue line), $\sigma = 0.15$ fb (blue line), $\sigma = 0.3$ fb (green line), $\sigma = 0.85$ fb (red line). The red-shadowed region is excluded by unitarity constraints.

suggesting the layout of figures 7-10. The work of all of us is supported in part by the NExT Institute.

-
- [1] A. Djouadi, Phys. Rept. **457**, 1 (2008), arXiv:hep-ph/0503172.
 - [2] E. E. Jenkins, Phys. Lett. **B192**, 219 (1987).
 - [3] W. Buchmuller, C. Greub, and P. Minkowski, Phys. Lett. **B267**, 395 (1991).
 - [4] S. Khalil, J. Phys. **G35**, 055001 (2008), arXiv:hep-ph/0611205.
 - [5] P. Minkowski, Phys. Lett. **B67**, 421 (1977).
 - [6] P. Van Nieuwenhuizen and D. Z. Freedman, 341(1979), amsterdam, Netherlands: North-Holland.
 - [7] T. Yanagida(1979), in Proceedings of the Workshop on the Baryon Number of the Universe and Unified Theories, Tsukuba, Japan, 13-14 Feb.
 - [8] M. Gell-Mann, P. Ramond, and R. Slansky print-80-0576 (CERN).

- [9] S.L. Glashow, in *Quarks and Leptons*, eds. M.Lèvy et al. (Plenum, New York 1980), p. 707.
- [10] R. N. Mohapatra and G. Senjanovic, Phys. Rev. Lett. **44**, 912 (1980).
- [11] W. Emam and S. Khalil, Eur. Phys. J. **C52**, 625 (2007), arXiv:0704.1395 [hep-ph].
- [12] L. Basso, A. Belyaev, S. Moretti, and C. H. Shepherd-Themistocleous, Phys. Rev. **D80**, 055030 (2009), arXiv:hep-ph/0812.4313.
- [13] W. Emam and P. Mine, J. Phys. **G36**, 129701 (2009).
- [14] K. Huitu, S. Khalil, H. Okada, and S. K. Rai, Phys. Rev. Lett. **101**, 181802 (2008), arXiv:0803.2799 [hep-ph].
- [15] L. Basso, A. Belyaev, S. Moretti, and G. M. Pruna, JHEP **10**, 006 (2009), arXiv:0903.4777 [hep-ph].
- [16] L. Basso, A. Belyaev, S. Moretti, G. M. Pruna, and C. H. Shepherd-Themistocleous(2010), arXiv:1002.3586 [hep-ph].
- [17] O. Bahat-Treidel, Y. Grossman, and Y. Rozen, JHEP **05**, 022 (2007), arXiv:hep-ph/0611162.
- [18] D. O’Connell, M. J. Ramsey-Musolf, and M. B. Wise, Phys. Rev. **D75**, 037701 (2007), arXiv:hep-ph/0611014.
- [19] V. Barger, P. Langacker, M. McCaskey, M. J. Ramsey-Musolf, and G. Shaughnessy, Phys. Rev. **D77**, 035005 (2008), arXiv:0706.4311 [hep-ph].
- [20] G. Bhattacharyya, G. C. Branco, and S. Nandi, Phys. Rev. **D77**, 117701 (2008), arXiv:0712.2693 [hep-ph].
- [21] S. Profumo, M. J. Ramsey-Musolf, and G. Shaughnessy, JHEP **08**, 010 (2007), arXiv:0705.2425 [hep-ph].
- [22] V. Barger, P. Langacker, M. McCaskey, M. Ramsey-Musolf, and G. Shaughnessy, Phys. Rev. **D79**, 015018 (2009), arXiv:0811.0393 [hep-ph].
- [23] L. Basso, A. Belyaev, S. Moretti, and G. M. Pruna, Phys. Rev. **D81**, 095018 (2010), arXiv:1002.1939 [hep-ph].
- [24] L. Basso, S. Moretti, and G. M. Pruna, Phys. Rev. **D82**, 055018 (2010), arXiv:1004.3039 [hep-ph].
- [25] L. Basso, S. Moretti, and G. M. Pruna(2010), arXiv:1009.4164 [hep-ph].
- [26] S. Dawson and W. Yan, Phys. Rev. **D79**, 095002 (2009), arXiv:0904.2005 [hep-ph].
- [27] G. Cacciapaglia, C. Csaki, G. Marandella, and A. Strumia, Phys. Rev. **D74**, 033011 (2006), arXiv:hep-ph/0604111.

- [28] P. L. Anthony *et al.* (SLAC E158), Phys. Rev. Lett. **92**, 181602 (2004), arXiv:hep-ex/0312035.
- [29] The ALEPH, DELPHI, L3, OPAL, SLD Collaborations, the LEP Electroweak Working Group, the SLD Electroweak and Heavy Flavour Groups (LEP)(2003), arXiv:hep-ex/0312023.
- [30] P. Azzi *et al.* (CDF and D0 and Tevatron Electroweak Working Group)(2004), arXiv:hep-ex/0404010.
- [31] M. Woods (SLAC E158)(2004), arXiv:hep-ex/0403010.
- [32] The ALEPH, DELPHI, L3, OPAL, SLD Collaborations, the LEP Electroweak Working Group, the SLD Electroweak and Heavy Flavour Groups, Phys. Rept. **427**, 257 (2006), hep-ex/0509008.
- [33] M. S. Carena, A. Daleo, B. A. Dobrescu, and T. M. P. Tait, Phys. Rev. **D70**, 093009 (2004), arXiv:hep-ph/0408098.
- [34] T. Aaltonen *et al.* (CDF), Phys. Rev. Lett. **102**, 031801 (2009), arXiv:0810.2059 [hep-ex].
- [35] T. Aaltonen *et al.* (CDF), Phys. Rev. Lett. **102**, 091805 (2009), arXiv:0811.0053 [hep-ex].
- [36] G. L. Fogli *et al.*, Phys. Rev. **D78**, 033010 (2008), arXiv:0805.2517 [hep-ph].
- [37] A. Pukhov(2004), arXiv:hep-ph/0412191.
- [38] A. V. Semenov(1996), arXiv:hep-ph/9608488.
- [39] J. F. Gunion, H. E. Haber, G. L. Kane, and S. Dawson, *THE HIGGS HUNTER'S GUIDE* (Addison Wesley, 1990).
- [40] D. Graudenz, M. Spira, and P. M. Zerwas, Phys. Rev. Lett. **70**, 1372 (1993).
- [41] M. Spira, A. Djouadi, D. Graudenz, and P. M. Zerwas, Nucl. Phys. **B453**, 17 (1995), arXiv:hep-ph/9504378.
- [42] R. Barate *et al.* (LEP Working Group for Higgs boson searches), Phys. Lett. **B565**, 61 (2003), arXiv:hep-ex/0306033.
- [43] P. Fileviez Perez, T. Han, and T. Li, Phys. Rev. **D80**, 073015 (2009), arXiv:0907.4186 [hep-ph].
- [44] D. M. Asner *et al.*(2010), arXiv:1004.0535 [hep-ph].
- [45] L. Basso, A. Belyaev, S. Moretti, and G. M. Pruna(2011), in progress.
- [46] T. Cuhadar-Donszelmann, M. Karagoz, V. E. Ozcan, S. Sultansoy, and G. Unel, JHEP **10**, 074 (2008), arXiv:0806.4003 [hep-ph].